J Therm Anal Calorim (2010) 100:493–500
DOI 10.1007/s10973-009-0652-9

A fully automatic apparatus for thermal analysis of crystallization from solution and metastable zone width determinations

Carlos E. S. Bernardes · Manuel E. Minas da Piedade

Portuguese Special Chapter
Received: 22 September 2008 / Accepted: 18 March 2009 / Published online: 12 January 2010

Abstract This work describes the development of a fully automatic apparatus to perform crystallization studies and metastable zone width (MSW) determinations using the polythermal method. Heating and cooling ramps, and isothermal steps can be carried out, while continuously monitoring the mixture inside the crystallization vessel, with temperature and turbidity sensors. These allow the onsets of crystallization or of complete dissolution of the solute to be detected. Programmed dilutions of the mixture under study can also be automatically performed, so that different concentrations can be studied in a given experiment. The apparatus was tested by using the ammonium chloride–water system. The results indicated that it is capable of reproducing the equilibrium solubilities of ammonium chloride in water, independently determined by the residue mass method, with an average deviation of 0.6 K. The obtained MSW and the kinetic parameters for the crystallization process showed deviations from the literature data, which are typical of these studies when nucleation is not induced by the addition of crystalline seeds.

Keywords Thermal analysis · Crystallization · Solubility · Metastable zone width · Turbidity · Ammonium chloride

Introduction

Crystallization from solution has been used as a purification method since the dawn of civilization. Despite this fact, it is still one of the most important techniques for obtaining compounds with a high degree of purity [1]. The method is equally used in research laboratories and in industry. The applications range from large scale production or recovery of solid materials, to more specialized goals, such as the isolation of new substances, or the selective preparation of different crystalline phases (polymorphs) or solvates of a given compound [1–3]. The synthesis of stable polymorphs and solvates currently has, for example, a strong impact in the pharmaceutical industry, since it provides a means to alter the properties of an active principle (e.g., the dissolution rate which often determines the bioavailability) in view of an application, without changing the molecule involved [2, 3]. The control of the crystallization kinetics also allows, to a certain extent, the production of materials with optimum crystal sizes and size distributions for further use or processing [1, 4].

Thermal analysis is a powerful method to study several aspects of crystallization from solution. The designation thermal analysis generally applies to techniques where physical or chemical changes in a given sample are monitored as a function of a programmed temperature–time variation [5]. Thermal analytical methods are, therefore, very convenient to evaluate how the onsets of crystallization (limit of supersaturation) or complete dissolution of crystalline materials depend on cooling or heating rates, and to provide information about the kinetics of those processes.

Crystallization of a solute is usually accompanied by the evolution of heat (the enthalpy of crystallization for a process at constant pressure), which causes a rise in the temperature of the solution. Hence, if a solution is cooled at a controlled rate, crystallization may be detected by a sudden temperature change with the onset at a specific temperature. This temperature is normally taken as the nucleation temperature, T_n, (i.e., the temperature

C. E. S. Bernardes · M. E. M. da Piedade (✉)
Departamento de Química e Bioquímica, Faculdade de Ciências, Universidade de Lisboa, 1649-016 Lisbon, Portugal
e-mail: memp@fc.ul.pt

corresponding to the formation of the smallest stable molecular aggregates necessary for the development of the macroscopic crystals), although the detected solid may be formed by entities that have already undergone some growing beyond nuclei dimensions. A similar procedure allows the determination of the minimum temperature for complete solubilization of a suspension of the material under study on heating at a constant rate. This may be a very good approximation of the equilibrium saturation temperature, T_s, if significant departures from equilibrium are not created by the dynamic nature of the temperature rise. The thermal changes associated with precipitation or dissolution may be small and difficult to observe. Therefore, it is always convenient to also monitor the beginning of crystallization by using non-thermometric probes such as a ultrasonic velocity [6], or a turbidity detector [7].

Since supersaturation (a solution is said to be supersaturated at a given temperature, if it contains a larger concentration of dissolved solid than that corresponding to the equilibrium saturation at that temperature) is an essential requirement for the crystallization to occur, the values of T_n and T_s for a given concentration, c, are not coincident. Their difference establishes the limits of the metastable zone width (MZW) [1, 4], which can be evidenced in a saturation–supersaturation diagram, such as that illustrated in Fig. 1 for a substance whose solubility increases with the temperature. The lower curve (solid line), gives the variation of the equilibrium solubility with the temperature, which can normally be accurately and reproducibly determined by a variety of methods [1]. The upper supersaturation curve (dashed line) represents the temperatures and concentrations at which spontaneous crystallization is observed, and its position in the graph is strongly affected by several experimental factors. In practice, some of these, such as the cooling or stirring rates, are easy to keep under tight control, but others, such as the presence of trace impurities and ambient dust are much more prone to erratic changes [1]. Three zones are apparent in the diagram of

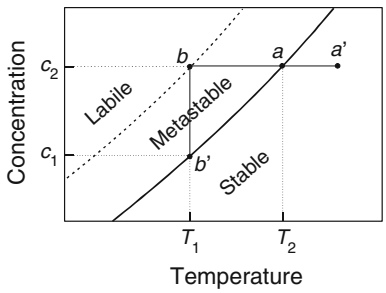

Fig. 1 Saturation–supersaturation diagram showing the stable, metastable, and labile zones for the crystallization of a solid from solution. The *solid line* represents the equilibrium solubility curve and the *dashed line* represents the maximum supersaturation or nucleation curve. The separation of the two curves represents the metastable zone width

Fig. 1: (i) The stable unsaturated zone, on the right, where crystallization cannot occur; (ii) the metastable supersaturated zone, in the middle, where spontaneous crystallization on a reasonably short time is improbable, but may occur if a crystal seed is introduced in the solution; and (iii) the labile or unstable supersaturated zone, on the left, where spontaneous crystallization is expected to occur. The saturation curve establishes a well-defined limit between the unsaturated and metastable zones. The metastable-labile boundary may change, however, to some extent, due to the above mentioned dependence of the supersaturation curve on a multiplicity of experimental variables, some of which are difficult to control in practice.

According to the classical theory of nucleation, for each degree of supersaturation, nuclei of a certain critical size are in equilibrium with the surrounding solution and have the same probability of growth as of decomposition [1, 4, 8]. Aggregates smaller than the critical size tend to fall apart, and those larger than the critical size tend to grow spontaneously. The rates of nucleation and of crystal growth following nucleation depend on the degree of supersaturation. Thus, once the MZW is known for a convenient set of experimental conditions (cooling rate, stirring, etc.), it is possible to devise a crystallization protocol where a constant supersaturation is approximately maintained throughout the cooling, leading to nearly constant nucleation and crystal growth rates [9, 10]. This allows some control of the nucleation and crystal growth kinetics and, therefore, of the optimum crystal size and size distribution, which, as mentioned above, may be important for further use or processing of the obtained product [1, 4].

The polythermal method introduced by Nývlt [4] is perhaps the most commonly used technique to determine saturation–supersaturation diagrams similar to that in Fig. 1. The basis of the method can be outlined by referring again to Fig. 1. First, a solution, a', of known concentration c_2, is cooled at a constant rate, β, until the formation of solid is observed at the temperature, T_1 (point b). This temperature is taken as the nucleation temperature. The obtained solid suspension is subsequently heated at the same rate until complete dissolution of the crystals is noted at point a. The corresponding temperature T_2 is assumed to be the equilibrium saturation temperature. The final solution is diluted to a concentration c_1, and the process is repeated until a sufficient number of points have been collected to define the equilibrium solubility (solid line) and the supersaturation (dashed line) curves. The limits of the MSW are defined by the maximal attainable supersaturation $\Delta c_{max} = c_2 - c_1$ or the corresponding maximal attainable supercooling $\Delta T_{max} = T_2 - T_1$.

Due to the dependence of the nucleation rate on supersaturation, studies by the polythermal method also provide a means to obtain information about the kinetics of

crystallization. Although various theories have been introduced to rationalize the nucleation kinetics, e.g., [1, 4, 8], the intrinsic complexity of the process and various experimental limitations, make the routine application of those theories to data analysis difficult in most cases. Note, for example, that the structure of the critical nucleus for a given supersaturation is virtually impossible to establish and the extent of nuclei growing beyond the critical size previous to detection, may strongly depend on the selected detection method. Therefore, empirical approaches are most often preferred to analyze the kinetics of crystallization. In this case, the mass nucleation rate, J, is typically expressed by [1, 4]

$$J = k_{\mathrm{n}} \Delta c_{\max}^{n} \tag{1}$$

where $\Delta c_{\max}$ is the MSW for a given temperature, k_{n} is the nucleation rate constant, and n is the nucleation order. Analogously to the reaction order for complex chemical processes [11], n is a purely empirical parameter which bears no relation to the nucleation molecularity, i.e., the number of molecules involved in the critical nuclei formation. Since J has been defined as the mass nucleation rate in the following discussion, it will be considered that the concentrations, c, used to calculate $\Delta c_{\max}$ are expressed in mass of solute per a given mass of solvent. It will also be assumed and that no solvates crystallize from the solution.

If the section of the MTW considered is not too large, it is normally reasonable to suppose that the saturation and supersaturation lines are linear and parallel (Fig. 1). Hence,

$$\Delta c_{\max} = \frac{\mathrm{d}c_{\mathrm{s}}}{\mathrm{d}T} \Delta T_{\max} \tag{2}$$

where $\mathrm{d}c_{\mathrm{s}}/\mathrm{d}T$ represents the slope of the equilibrium solubility line, equal to that of the supersaturation line $\mathrm{d}c_{\mathrm{ss}}/\mathrm{d}T$. Further assuming that the mass nucleation rate equals the rate of solution supersaturation, at least when the nucleation is detected, then

$$J = \frac{\mathrm{d}c_{\mathrm{s}}}{\mathrm{d}T} \beta \tag{3}$$

where $\beta = |\mathrm{d}T/\mathrm{d}t|$ is the absolute value of the cooling rate.

Combining Eqs 1–3 it is possible to conclude that

$$\log \Delta T_{\max} = \frac{1-n}{n} \log\left(\frac{\mathrm{d}c_{\mathrm{s}}}{\mathrm{d}T}\right) - \frac{1}{n} \log k_{\mathrm{n}} + \frac{1}{n} \log \beta \tag{4}$$

According to Eq 4, a plot of $\log \Delta T_{\max}$ against $\log \beta$ should give a straight line whose slope a and intercept b are related to the nucleation order and the rate constant of the crystallization process through

$$n = \frac{1}{a} \tag{5}$$

$$\log k_{\mathrm{n}} = (1-n) \log\left(\frac{\mathrm{d}c_{\mathrm{s}}}{\mathrm{d}T}\right) - nb \tag{6}$$

The term $\mathrm{d}c_{\mathrm{s}}/\mathrm{d}T$ is constant for a given concentration and can be obtained from the saturation line. Therefore, once a and b are known, n and k_{n} can readily be derived from Eqs. 5 and 6. Since the slope of Eq. 4 depends only on the nucleation order, the representations of $\log \Delta T_{\max}$ versus $\log \beta$ for different concentrations should give parallel lines. It has, therefore, been recommended that the $\log \Delta T_{\max}$ versus $\log \beta$ data obtained for all the concentrations studied should be globally fitted as a system of j parallel straight lines, using a modified least squares method [4]. The slope A of these lines and their individual intercepts B_j are given by

$$A = \frac{\sum_{j=1}^{p} \left[\sum_{i=1} x_i y_i - \sum_{i=1} \frac{x_i}{N_j} \cdot \sum_i y_i \right]_j}{\sum_{j=1}^{p} \left[\sum_i x_i^2 - \frac{\left(\sum_i x_i \right)^2}{N_j} \right]_j} \tag{7}$$

$$B_j = \frac{\left(\sum_i y_i - A \sum_i x_i \right)_j}{N_j} \tag{8}$$

were $x_i = \log \beta$, $y_i = \log \Delta T_{\max}$, p is the total number of linear relations considered, and N_j is the number of measurements carried out for each line j.

In spite of some severe underlying approximations [1, 4], Eq 4 is still regarded as a useful means of characterizing the metastability of crystallizing systems and their crystallization kinetics, at least for industrial applications [6, 12, 13].

Here, we describe the construction and test of a fully automatic reactor for crystallization studies by the polythermal method. The apparatus was tested by using the crystallization of ammonium chloride from water. Ammonium chloride was selected for this role because it is commercially available in a high degree of purity at a relatively low price, and is stable for years if stored in a cool dry place. Furthermore, complicating effects due to the concomitant formation of hydrates during crystallization are absent [1], and equilibrium solubility and MSW data are available for comparison [1, 4, 14].

Experimental

Materials

Ammonium chloride (Panreac, PA-ACS-ISO, 99.5%) was used as received. Water (conductivity, < 0.1 μS cm^{-1}) was distilled and deionized in a Millipore system, previously to the experiments.

Equilibrium solubility measurements

The equilibrium solubility curve of ammonium chloride in water in the range 294.79–332.43 K was determined by the residue mass technique [15]. In a typical experiment, a saturated aqueous solution of NH_4Cl was prepared, under nitrogen atmosphere, inside a 250 cm^3 jacketed glass cell. The temperature of the mixture was maintained constant to better than ±0.05 K, by circulating water from a thermostatic bath through the outer jacket of the cell. The temperature of the bath was controlled by a JULABO F25-EC unit. Temperature measurements were performed with an accuracy of ±0.01 K using a Pt100 sensor immersed in the mixture and connected in a four wire configuration to an Agilent 34970A multimeter. The sensor had been previously calibrated against another platinum resistance thermometer, which in turn had been calibrated at an accredited facility in accordance to the International Temperature Scale ITS-90. The mixture was maintained under magnetic stirring, using a Teflon-coated stirring bar, for at least 8 h, to ensure that the solid in suspension and the solution were in equilibrium. A sample of the solution (~2 cm^3) was transferred to a vial of known mass, by using a syringe adapted to a Schleicher & Schuell BA 65 membrane filter (45 μm, i.d. 25 mm). In order to avoid precipitation, the syringe and membrane filter were kept in an oven whose temperature was set to ~10 K above the temperature of the solution, prior to use. The mass of solvent (m_{solv}) and the corresponding mass of NH_4Cl (m_{NH_4Cl}), were obtained by weighing the vial before and after solvent evaporation. The weightings were performed with a precision of ±0.01 mg with a Mettler Toledo XS205 balance.

Measurements by the polythermal method: the CB1 Apparatus

A general scheme of the apparatus dubbed CB1, developed in this work to study the MSW by the polythermal method, is shown in Fig. 2. The crystallization reactor, *1*, consists of a 100 cm^3 glass vessel, *2*, adapted to a stainless steel (AISI 316) head, *3*. The reactor is immersed in a JULABO F33-ME thermostatic bath, *4*, containing ethanol. The temperature of the bath can be varied at programmed rate. The head supports an Avantes FCR-71R200-2-45-ME turbidity probe, *5*, a platinum resistance thermometer (Pt100), *6*, a 4-blade 45°-pitched turbine glass impeller, *7*, and a 0.60 mm ID, 0.91-mm OD steel needle, *8*, that is used for solvent dispensing. The turbidity probe *5* introduces light from an Avantes HL-6000S source, *9*, into the reactor and also collects the dispersed light, which is then analyzed by an Avantes AvaSpect 2048 spectrophotometer, *10*. A fiber optics system connects the probe to the light source and spectrophotometer. The platinum resistance thermometer, *6*, is connected in a four wire configuration to an Agilent 34970A multimeter, *11*. It was calibrated as described for the temperature probe used in the residue mass measurements. The glass impeller is drive by a Wiggen Hauser BDC2000R motor, *12*, that controls the stirring rate to better than ±1 rpm. The concentration of the solution can be changed by adding solvent from the storage flask, *13*, through the needle, *8*, using a Crison Burette 1S automatic burette, *14*. The volume additions have a precision better than ±1 μL, as experimentally confirmed in a series of test runs with water. Before entering the reactor, the solvent travels through 2.5 m of 0.80 mm ID, 1.5-mm OD Teflon tube, wind around the five tubular pillars connecting the upper and bottom parts of the reactor head. This ensures that the solvent is dispensed at the temperature of the thermostatic bath fluid. Finally, a computer, *15*, controls all steps of the experiments and the data acquisition, by means of a software package also developed in this work.

In a typical experiment, the reactor was initially loaded with 32 cm^3 of a 49 g NH_4Cl/100 g H_2O solution. Both the solvent and the solute were weighted inside the glass vessel *2*, with a precision of ±0.1 mg, using a Mettler Toledo XS205 balance. The apparatus was assembled as shown in Fig. 2 and stirring was started at a desired rate (300 rpm in this case). The stirred mixture was subjected to a programmed temperature change as illustrated in Fig. 3. The initial suspension (point A) was heated at a constant rate, *β*,

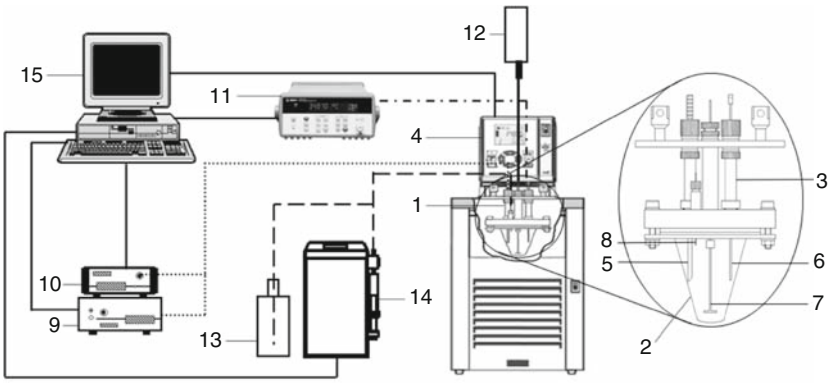

Fig. 2 Scheme of the crystallization apparatus: *1* crystallization reactor; *2* glass vessel; *3* stainless steel head. *4* thermostatic bath; *5* turbidity probe; *6* platinum resistance thermometer; *7* glass impeller; *8* steel needle; *9* light source; *10* spectrophotometer; *11* multimeter; *12* stirring motor; *13* solvent dispenser container; *14* automatic burette; *15* computer

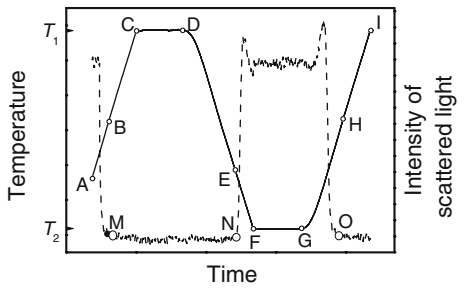

Fig. 3 Temperature-time curve (*solid line*) and corresponding turbidity curve (*dashed line*) obtained in a typical experiment with the CB1 apparatus

to the temperature T_1 (point C), which is 5 K higher than the solubilization temperature (point B). The complete dissolution of the solid was concomitant with a drop of the intensity of the scattered light to the baseline (point M). To minimize memory effects, the solution was left for 40 min at T_1 (isothermal step between points C and D) and subsequently cooled at the rate β to a temperature T_2 (point F) 5 K lower than the nucleation temperature T_n (point E). The formation of crystals was accompanied by a rapid increase of the scattered light intensity (point N). A new 40 min isothermal step was performed at T_2 (between points F and G) followed by a heating ramp at the same rate β used in the cooling stage. The heating was stopped (point I) 5 K above the temperature of complete dissolution of the solid (point H). The value of T_s corresponding to point H was taken as the "equilibrium" saturation temperature. After reaching point I, a new isothermal step of 40 min was performed, and the cooling/heating sequence between points D and I was repeated for a different value of β, leading to new values of T_s and T_n. In the present work rates of 12, 18, 24, 30 and 36 K h^{-1} were used. When the experiments at each of these five β values were completed, the solution was automatically diluted by adding 2 cm^3 of water from the burette 14 (Fig. 2) and the described procedure was repeated for the new concentration. In this work the dilutions were performed until a concentration of $\sim$37 g of NH_4Cl/100 g of H_2O was reached.

The spectrophotometer used in the CB1 apparatus has a diode array detector, which enables the simultaneous acquisition of the full spectrum of the scattered light in the wavelength range 490–1024 nm. In this work, the scattered intensity was analyzed at 550, 600, and 650 nm. The average values of the solubilization and nucleation temperatures determined from the data recorded at these three wavelengths for each concentration and cooling/heating rates, were taken as the saturation, T_s, and nucleation, T_n, temperatures, respectively.

Since the dilutions were volumetrically performed, the massic concentrations of the NH_4Cl solutions (expressed as mass of anhydrous solute by mass of solvent) were based on the mass of added water m (in grams) calculated from:

$$m = V(-1.44510 \times 10^{-10}\, T^4 + 2.02215 \times 10^{-7}\, T^3 - 1.08687 \times 10^{-4}\, T^2 + 2.59474 \times 10^{-2}\, T - 1.29515) \quad (9)$$

where V is the corresponding volume (in cm^3), and T (in K) is the temperature of the thermostatic fluid. Equation 9 was derived from the reported values of the density of pure water in the range 273–373 K [16].

Results and discussion

The equilibrium solubilities of NH_4Cl in water, determined by the residue mass method in the range 294.79–332.43 K are summarized in Table 1. The indicated uncertainties correspond to the mean deviation of three independent measurements. A polynomial least squares fit to the data in Table 1 led to the equation

$$c_{NH_4Cl} = 1.754 \times 10^{-3} T^2 - 0.6540T + 78.83 \quad (10)$$

where c_{NH_4Cl} is the concentration of NH_4Cl in g/100 g H_2O, and T represents the temperature in K. The obtained results are compared in Fig. 4, with recommended literature values [1], which correspond to the equation

$$c_{NH_4Cl} = 1.000 \times 10^{-3}\, T^2 - 0.1763T + 2.945 \quad (11)$$

The c_{NH_4Cl} values, calculated form Eqs. 10 and 11 in the temperature range covered by the experiments, show mean and maximum deviations of 0.7 and 1.4%, respectively. In general, this difference is within the experimental error of the determinations. It should be noted that the agreement between the two series of data would be even more favorable if the uncertainties of the literature data were known.

The solubilization, T_s, and nucleation, T_n, temperatures for the NH_4Cl–H_2O system, determined with the CB1

Table 1 Equilibrium solubilities of ammonium chloride in water at different temperatures determined by the residue mass method

T/K	c_{NH_4Cl}/(g/100g)
294.79	38.25 ± 0.25
295.79	38.80 ± 0.26
302.44	41.48 ± 0.05
303.42	42.24 ± 0.67
309.92	44.69 ± 1.38
310.74	44.56 ± 0.08
316.51	47.57 ± 0.02
321.62	49.73 ± 0.19
332.43	55.29 ± 0.46

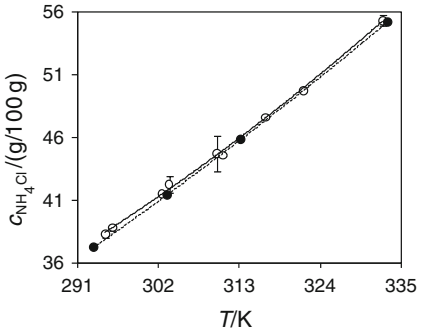

Fig. 4 Solubility of ammonium chloride in water obtained in this work by the residue mass method (*open circle*) and recommended in Ref. [1] (*filled circle*)

apparatus are shown in Table 2. For comparison purposes, the data were fitted to second order polynomial equations of the type

$$c_{NH_4Cl} = aT^2 + bT + c \quad (12)$$

and the obtained coefficients for each value of the heating/cooling rate, β, are given in Table 3. The differences, ΔT_s, between the solubility temperatures calculated from these fittings for selected concentrations and the corresponding equilibrium solubilities given by Eq. 10, are summarized in Table 4. It can be concluded from Table 4 that, in most cases, the values of T_s obtained with the CB1 apparatus are slightly lower than the equilibrium values determined by the residue mass method (negative ΔT_s values). This is not unexpected due to the dynamic nature of the measurements made with the reactor. The absolute values of ΔT_s vary in the range 0.01–1.19 K, the mean being 0.6 K. No clear tendency for a variation of ΔT_s with the concentration and heating rate is noted. The results, therefore, indicate that

Table 3 Constants a, b, and c, and regression coefficients R obtained by fitting Eq. 12 to the data in Table 2

β/K h^{-1}	a	b	c	R
Solubility				
12	1.238×10^{-3}	-3.474×10^{-1}	33.40	0.999
18	1.024×10^{-3}	-2.016×10^{-1}	8.625	1.000
24	8.237×10^{-4}	-7.535×10^{-2}	−11.20	0.999
30	1.161×10^{-3}	-2.874×10^{-1}	22.02	0.999
36	7.985×10^{-4}	-6.764×10^{-2}	−11.26	0.999
Nucleation				
12	3.120×10^{-3}	−1.477	204.5	0.989
18	3.385×10^{-3}	−1.657	235.1	0.996
24	-2.014×10^{-3}	1.601	−255.7	0.990
30	-1.227×10^{-3}	1.110	−179.2	0.987
36	-1.688×10^{-3}	1.387	−220.1	0.984

Table 2 Solubilization, T_s, and nucleation, T_n, temperatures of ammonium chloride in water for different cooling and heating rates, β, and concentrations, c_{NH_4Cl}, obtained with the CB1 apparatus

c_{NH_4Cl}/(g/100g)	β/K h^{-1}									
	12		18		24		30		36	
	T_n/K	T_s/K	T_n/K	T_s/K	T_n/K	T_s/K	T_n/K	T_s/K	T_n/K	T_s/K
49.383	315.64		315.98		317.82		317.47		317.50	
49.264		320.32	315.82	320.44	315.99	320.36		320.81	313.73	321.01
48.422						318.41	313.26	318.47	310.65	318.58
46.520		314.48	308.30	314.35	306.10	314.71	308.14	314.71	308.27	314.57
46.408		314.02		314.28		313.66		314.34	307.31	314.47
46.381		314.52		314.57	305.59	314.58	304.62	314.50	303.94	314.62
46.292		314.13		314.23		314.04		314.16		314.33
44.343		308.58		309.24				309.68		309.53
43.962	305.62		305.00		303.64	308.00	303.47	307.94	300.53	308.74
43.857		307.88	303.23	308.02		308.41		308.28		308.52
43.845		308.46	304.21			308.61	301.92	308.50		308.63
41.664	298.61	301.92	297.40	302.97	298.10	302.74	296.57	303.32	297.91	302.45
41.567	295.46	302.99		303.19		302.47	292.74	303.17	291.53	303.23
41.567	299.09			303.24		303.22		303.24		302.99
41.567										303.20
39.590	292.43	297.70	291.19	298.12	291.16	298.26	291.83	298.33	289.86	298.43
39.508	292.73		289.82	298.24	289.79	298.24	289.03	298.32	287.53	298.32
39.501					290.20	298.20		298.03		297.60
37.711	288.89	292.61	286.19	293.52	286.43	293.64	285.38	293.28	284.99	293.76

Table 4 Differences, ΔT_s, between the solubilities determined with the CB1 apparatus and calculated from Eq. 12 and Table 3, and the equilibrium solubilities given by Eq. 10

β/K h^{-1}	ΔT_s/K					
	c_{NH_4Cl}/(g/100g)					
	47	45	43	41	39	37
12	–0.73	–0.91	–1.05	–1.15	–1.19	–1.16
18	–0.56	–0.61	–0.58	–0.48	–0.28	0.05
24	–0.71	–0.76	–0.71	–0.56	–0.28	0.15
30	–0.47	–0.52	–0.51	–0.43	–0.27	–0.01
36	–0.40	–0.53	–0.56	–0.50	–0.30	0.04

Table 5 Maximum undercooling or metastable zone width, ΔT_{max}, obtained with the CB1 apparatus for different concentrations, c_{NH_4Cl}, and cooling rates, β

β/K h^{-1}	ΔT_{max}/K					
	c_{NH_4Cl}/(g/100g)					
	47	45	43	41	39	37
12	4.27	4.04	3.97	4.12	4.60	5.54
18	5.00	5.11	5.50	6.28	7.63	9.89
24	5.64	6.60	7.16	7.39	7.30	6.93
30	5.66	6.74	7.49	7.94	8.09	7.95
36	7.67	8.66	9.30	9.61	9.62	9.35

the CB1 reactor is capable of reproducing the equilibrium solubilities of NH_4Cl in water with an accuracy better than 0.4%.

The nucleation temperatures calculated from the coefficients in Table 3 and Eq. 12 are compared in Fig. 5 with the equilibrium solubilities measured by the residue mass method for the same temperature range. These were derived from Eq. 10.

Table 5 gives the maximum undercooling or MSW, ΔT_{max}, determined for the nucleation of NH_4Cl in water, with the CB1 apparatus. The ΔT_{max} values were calculated from Eq. 12 and the appropriate coefficients in Table 3. The results show that ΔT_{max} decreases with the decrease of the cooling rate and, in general, ΔT_{max} increases with the decrease of the saturation concentration. As shown in Table 6, the same trends are deduced from an analysis of published ΔT_{max} data for the same system. It can also be noted that, despite differences in experimental conditions, the ΔT_{max} values obtained in this work (Table 5) are systematically larger than the published ones (Table 6). This may, at least in part, result from the use of NH_4Cl samples with different purities in ours and other laboratories. Chianese et al. [14] showed that the addition of 150–300 ppm of Al^{3+}, Mn^{2+}, or Fe^{2+} to an aqueous solution of

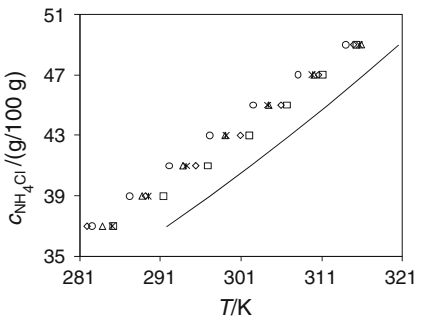

Fig. 5 Nucleation temperatures of ammonium chloride in water obtained with the CB1 apparatus at (*open circle*) 36, (*open triangle*) 30, (*asterisk*) 24, (*open diamond*) 18, and (*open square*) 12 K h^{-1}. The *solid line* represents the equilibrium solubility given by Eq. 10

Table 6 Metastable zone widths, ΔT_{max}, for the NH_4Cl–H_2O system reported in literature for different saturation temperatures, T_{sat} and cooling rates, β

T_{sat}/K	β/K h^{-1}	ΔT_{max}/K	Reference
298.15	5	0.7	[1]
303.15	5	1.43	[4]
303.15	20	1.83	[4]
333.15	5	0.99	[4]
333.15	20	1.27	[4]
324.15	30	1.85[a]	[14]
324.15	30	3.6[a,b]	[14]
324.15	30	4.0[a,c]	[14]
324.15	30	4.1[a,d]	[14]

[a] Average of two measurements using a stirring rate of 300 rpm, [b] in the presence of 150 ppm of Al^{3+}, [c] in the presence of 300 ppm of Fe^{2+}, [d] in the presence of 150 ppm of Mn^{2+}

NH_4Cl prepared from a 99.9% pure (mass percentage) sample increased ΔT_{max} by up to 1.7–2.3 K (see Table 6). Qualitatively this observation is consistent with the fact that larger ΔT_{max} values are obtained with the 99.5% pure sample used in our case, which according to the supplier contained trace amounts of several metal ion impurities, including iron (0.0002%), potassium (0.005%), calcium (0.001%), and sodium (0.005%).

The experimental data in Table 5 were fitted to Eq. 4 by using the modified regression method recommended by Nývlt et al. [4], mentioned in the "Introduction" section (see Eqs. 7 and 8). The obtained log ΔT_{max} versus log β plots are shown in Fig. 6, and the corresponding values of the A and B fitting parameters, the apparent nucleation order, n, and the nucleation rate constant k_n are summarized in Table 7. Equilibrium solubility data are normally tabulated in g solute/100 g solvent [1, 4] and, for comparison purposes, we have also followed this convention throughout this work. In the case of kinetic studies, however, it is preferable to express c_s as a mass fraction, because the units of k_n become independent of the nucleation order found (recall Eq. 1), thus

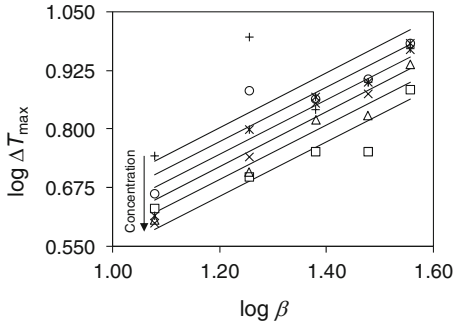

Fig. 6 Representation of log ΔT_{max} versus log β for different concentration of ammonium chloride in water: (*open square*) 47, (*open triangle*) 45, (*cross*) 43, (*asterisk*) 41, (*open circle*) 39 and (*plus*) 37 g/100 g

Table 7 Crystallization kinetics parameters for the NH_4Cl–H_2O system obtained in this work and reported in the literature, for different solute concentrations, c_{NH_4Cl}

Reference	c_{NH_4Cl}/(g/100g)	A[a]	B[a]	T_s[b]/K	log (k_n/h^{-1})	n
This work	37	0.584	0.102	290.9	1.56	1.71
	39	0.584	0.072	296.2	1.59	1.71
	41	0.584	0.045	301.3	1.62	1.71
	43	0.584	0.020	306.1	1.65	1.71
	45	0.584	−0.008	310.8	1.69	1.71
	47	0.584	−0.044	315.3	1.74	1.71
[4]				333.15	6.99	5.52
[4]				303.15	7.58	5.52

[a] Calculated from Eqs. 7 and 8

[b] Saturation temperatures for the corresponding concentration

facilitating comparisons between different determinations. For this reason, the values of dc_s/dT needed to calculate k_n through Eq. 6, were obtained from Eq. 10 with the coefficients divided by 100.

Also included in Table 7 are published n and k_n data for the NH_4Cl–H_2O system [4]. The analysis of Table 7 shows that the nucleation order and the kinetic constants reported in the literature are ca. three to five times higher than those obtained in this work. Differences of this magnitude are, however, not uncommon when studying MSWs in different laboratories, particularly when as in our case crystalline seeds are not used to induce crystallization. Note also that, as referred to above, factors such as the purity of the sample and the stirring rate may strongly influence ΔT_{max}. Since the purity of the sample and the stirring rate used to obtain the published results were not reported, they may not be strictly comparable to those obtained in this work.

Conclusions

The CB1 apparatus developed in this work was able to reproduce the equilibrium solubilities of ammonium chloride in water with a mean deviation of 0.6 K and the determination of the corresponding MSW for solute nucleation with an accuracy typical of these studies. After programming, the experiments can be performed under fully automatic operation, thus avoiding the need of constant supervision.

References

1. Mullin JW. Crystallization. 4th ed. Oxford: Butterworth-Heinemann; 2001.
2. Brittain HG. Polymorphism in pharmaceutical solids. New York: Marcel Dekker; 1999.
3. Bernstein J. Polymorphism in molecular crystals. Oxford: Oxford University Press; 2002.
4. Nývlt J, Söhnel O, Matuchová M, Broul M. The kinetics of industrial crystallization. Amsterdam: Elsevier; 1985.
5. Hemminger W, Sarge SM. Definitions, nomenclature, terms, and literature. In: Brown ME, editor. Handbook of thermal analysis and calorimetry, vol. 1. Amsterdam: Elsevier; 1998. p. 1.
6. Gürbüz H, Özdemir B. Experimental determination of the metastable zone width of borax decahydrate by ultrasonic velocity measurement. J Cryst Growth. 2003;252:343–9.
7. Sessiecq P, Gruy F, Cournil M. Study of ammonium chloride crystallization in a mixed vessel. J Cryst Growth. 2000;208:555–68.
8. Kashchiev D, van Rosmalen GM. Review: nucleation in solutions revisited. Cryst Res Technol. 2003;38:555–74.
9. Mullin JW, Nyvlt J. Programmed cooling of batch crystallizers. Chem Eng Sci. 1971;26:369–77.
10. Mayrhofer B, Nyvlt J. Programmed cooling of batch crystallizers. Chem Eng Process. 1988;24:217–20.
11. Leidler KJ. Chemical kinetics. 2nd ed. New York: Harper and Row; 1987.
12. Correia P, Lopes C, Minas da Piedade ME, Lourenço JAA, Serrano ML. Solubility and metastable zone width of 1-keto-1, 2, 3, 4-tetrahydro-6-methylcarbazole in acetone. J Chem Eng Data. 2006;51:1306–9.
13. Sahim O, Dolas H, Demir H. Determination of nucleation kinetics of potassium tetraborate tetrahydrate. Cryst Res Technol. 2007;42:766–72.
14. Chianese A, Santilli N, Sohnel O. Influence of admixtures and operating conditions on the crystallization of ammonium chloride. J Cryst Growth. 1996;166:1099–104.
15. Zimmerman HK. The experimental determination of solubilities. Chem Rev. 1952;51:25–65.
16. Lide DR. Handbook of chemistry and physics. 87th ed. Boca Raton: Taylor and Francis; 2007.